

GCEP award #40654: High-Efficiency, Low-Cost Thin Film Solar Cells

Alberto Salleo, *Dept. of Materials Science and Engineering, Stanford University*
Yi Cui, *Dept. of Materials Science and Engineering, Stanford University*
Peter Peumans, *Dept. of Electrical Engineering, Stanford University*

1. Motivation

The goal of the project is to develop materials and processing techniques that will allow the fabrication of low-cost multi-junction solar cells entirely by solution-processing or other low-cost techniques amenable to roll-to-roll (R2R) fabrication such as lamination. Device modeling will help identify the best device architecture. Integration of different types of materials (metals, oxides, semiconductors, polymers) is one of the goals of this project.

2. High-Efficiency, Low-Cost Multi-Junction Solar Cells

We propose to take advantage of nanostructured materials to fabricate high-efficiency multi-junction cells using solution-based processing techniques. As a result, our cells will be amenable to large-area fabrication, such as R2R, thereby dramatically reducing their cost. A crucial aspect of this technology is the introduction of transparent conducting materials that can be deposited in mild conditions in order to serve as intermediate electrodes in an unconstrained multi-junction architecture.

This report is divided in two sections: materials development, and integration in photovoltaic devices.

2-1 Materials development

2-1-1 ZnO

When comparing the electrical properties of doped ZnO nanostructures to those obtained in the bulk or by magnetron sputtering, a lower performance is observed which is potentially due to a limited incorporation and activation of the dopant atoms in the ZnO lattice. Therefore we study the mechanisms responsible for dopant inclusion and activation using a comprehensive set of spectroscopic techniques. A combination of optical absorption (photothermal deflection spectroscopy), anomalous X-ray diffraction, and nuclear magnetic resonance allow us to assess the effectiveness of the dopant addition.

Applying the Drude metal model to the absorption spectrum of these films measured using photothermal deflection spectroscopy (PDS) allows us to measure the electrical properties of nanowire ensembles as a function of doping and post-deposition treatments. Surprisingly, the free charge carrier absorption peak decreased with increasing annealing temperature, and modeling of these spectra resulted in nearly constant values in mobility and a slow decrease in charge density until a temperature close to 400°C, when the charge carriers completely disappear (Figure 1).

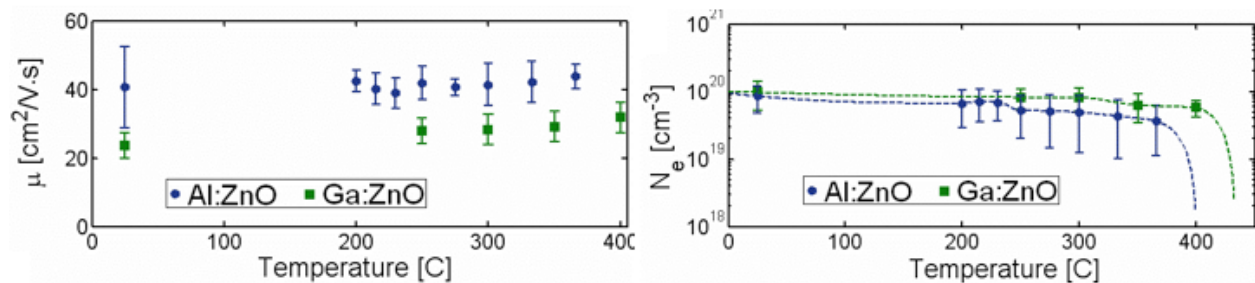


Figure 1: Carrier mobility and density in Al- and Ga-doped ZnO nanowires measured spectroscopically as a function of annealing temperature.

In order to study the coordination environment of dopants in the ZnO lattice, solid state Al NMR data and anomalous X-ray diffraction (AXRD) were used. NMR spectra indicate a far richer solid state chemistry that warrants further investigation, with the dopant occupying multiple lattice sites (Fig. 2). AXRD probes the presence of Ga atoms in the Wurtzite lattice sites by tracking changes in structure factor when scanning the X-ray photon energy across the Zn and Ga absorption edges, indicating a low incorporation of Ga into substitutional Zn sites, which is in good agreement with the amount of free charge observed in these materials.

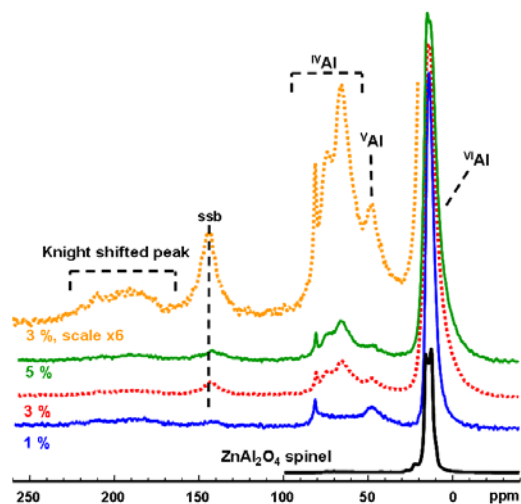


Figure 2: Solid-state Al NMR spectrum of Al-doped nanowires. The spectrum indicates the existence of four-fold, five-fold and six-fold coordinated Al atoms. The Knight shifted peak is related to the existence of free-charge in the nanowires.

In order to further enhance the functionality of ZnO electrode, we are studying light trapping properties of ZnO nanostructures. Improved electrical conductivity along with light trapping will give ZnO an edge over other transparent conductor technologies.

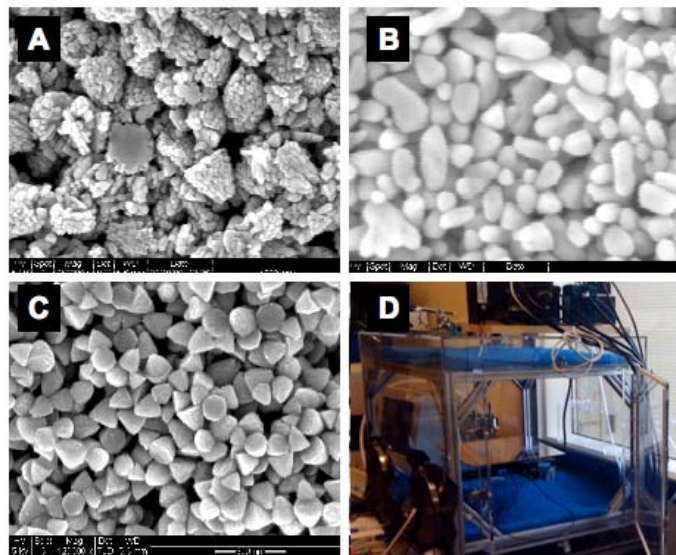


Figure 3: a) ZnO nanopylramids exhibiting 'fir-cone' like morphologies of aggregated small particles, grown in the presence of organic surfactant; the hexagonal-shape base is likely the [0001] crystal face of the wurtzite ZnO b) ZnO nanoparticles grown under the same conditions without any organic surfactant c) Ga-doped ZnO nanopylramids, grown under same experimental conditions, with an organic surfactant. Doped pyramids exhibit significantly higher surface uniformities compared to undoped ones d) Spray coating apparatus with pneumatic nozzle and automated X-Y stage

Hence we are exploring the light-diffusing properties of nanostructured ZnO films fabricated on glass substrates using a scalable, low-cost pneumatic spray coating process. Low-temperature synthesis of ZnO nanostructures with controlled size distributions and morphologies is achieved using solution-based synthesis process (Fig. 3a-c). Nanopyramid faces are observed to be rough, "fir-cone" like structures with 25 nm asperities. Nanopyramid thin films have exhibited promising light diffusing properties. Further SEM studies show that the incorporation of a Ga-dopant into nanopylramids results in smoother surfaces

thus enabling us to control their optical/electrical properties.

Pneumatic spray-coating is being investigated as a scalable, low-temperature deposition process of ZnO films from nanostructure precursor solutions (Fig. 3d). A spray coating apparatus was fabricated and designed for systematic optimization of deposition parameters. We demonstrate automated control of process variables including chamber pressure, nozzle pressure, nozzle raster velocities, deposition temperature, spraying distance, as well as solution flow rate. Currently, the spray deposition process is being optimized for obtaining uniform thin films. Further studies planned include quantification of effects of morphology, size and film annealing temperatures on the light diffusing properties and electrical conductivity.

Spray-coated ZnO nanostructures display outstanding light scattering properties. Preliminary measurements suggest haze factors as high as 0.4 in the near-infrared (Fig. 4).

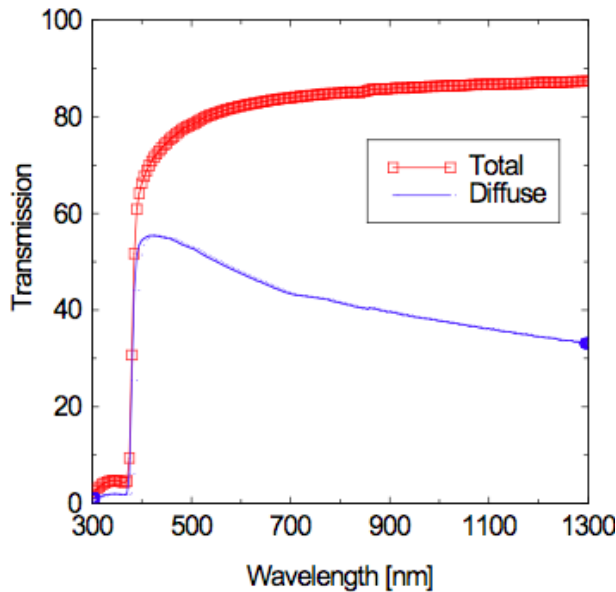


Figure 4: Total and diffuse transmission spectra of a spray-coated ZnO nanoparticle film. The ratio of the two curves is the haze factor.

2-1-2 Ag nanowire meshes

We have carried out a comprehensive study of transparent and conductive silver nanowire (Ag NW) electrodes, including the scalable fabrication process (Fig. 5), morphology studies, optical properties, mechanical adhesion and flexibility, and various routes to improve the performance.

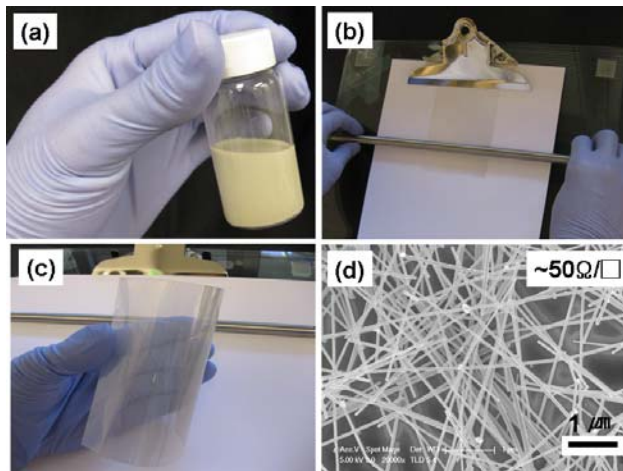


Figure 5: (a) Ag NW ink in ethanol solvent, with concentration of 2.7 mg/mL. (b) Meyer rod coating set up for scalable Ag NW coating on plastic substrate. The plastic substrate PET is put on a flat glass plate and a meyer rod is pulled over the ink and substrate, which leaves a uniform layer of Ag NW ink with thickness ranging from 4 μm to 60 μm . (c) Finished Ag NW film coating on PET substrate. The Ag NW coating looks uniform over the entire substrate shown in the figure. (d) A SEM image of Ag NW coating on as shown in (c). The sheet resistance is $\sim 50 \Omega/\square$.

We achieved control over the synthesis of long and thin wires for improved performance in terms of sheet resistance and optical transmittance. We achieved $20 \text{ } \Omega/\text{sq}$ and $\sim 80\%$ specular transmittance, and $8 \text{ } \Omega/\text{sq}$ and 80% diffusive transmittance in visible range, which falls in the same range of the best Indium Tin Oxide (ITO) films on plastic substrate for flexible electronics and solar cells. The Ag NW network exhibits a larger optical haze when compared with ITO and carbon nanotube electrodes due to the light scattering, which could greatly enhance the solar cell performance.

We have studied the electrical conductance of Ag nanowires and their junctions, and developed a method of Au coating (Fig. 6) to greatly enhance the junction conductance for better overall film conductance. The overall characterization of transparent Ag NW electrode meet the requirement as transparent electrode which could be an immediate replacement for ITO for plastic electronics and solar cells.

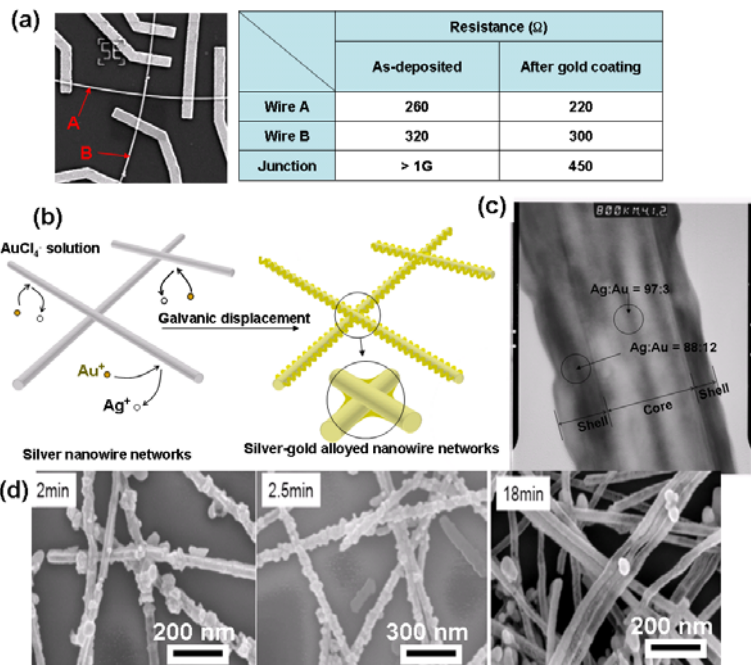
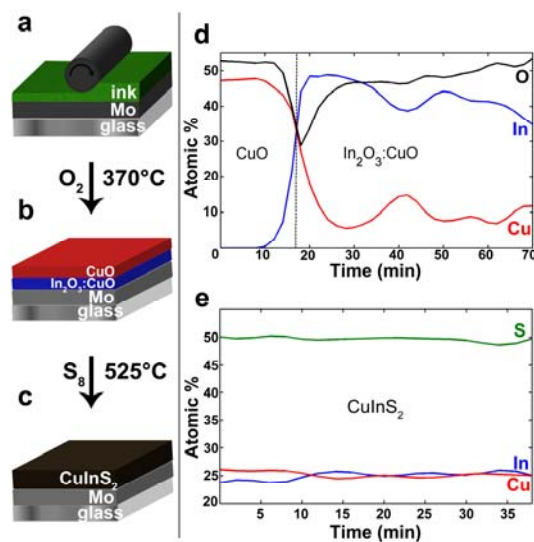


Figure 6: (a) Electrical measurement of individual Ag NWs and a junction. The junction shows much higher resistance than that of wires themselves. The junction resistance dramatically decreases from $>1 \text{ G } \Omega$ to $450 \text{ } \Omega$ after Au coating. The length of the two wires is $\sim 10 \text{ } \mu\text{m}$. (b) Schematic of Au-Ag alloy network formation with solution process. (c) TEM image showing the nanowire after the Au replacement. (d) Au replacement with different Au addition time. The surface of nanowires is smoother when Au is supplied slowly.

2-1-3 Active material: CuInS_2

We have initiated the development of air-stable ink rolling (AIR) process to produce film of CuInS_2 solar absorber layers. This process might produce flat and dense film and free of organic or carbon contamination, which has been one of the challenges in nanocrystal solar cell films. The process consist of the following steps (show in Figure 7) (a) Ink deposition process using roller-bar. (b) Oxide bilayer formation after heating at 370°C in air. (c). Film after sulfurization in sulfur vapor at 525°C . AES depth profile of oxide film showing segregation into a $\text{CuO}/\text{In}_2\text{O}_3:\text{CuO}$ bilayer and CuInS_2 film after sulfurization and KCN etching.



2-2 Integration in photovoltaic devices

In order to test their performance in devices, we fabricated photovoltaic cells with both Ag nanowire and ZnO nanowire electrodes. We used organic bulk heterojunction cells as a test bed because their behavior is well-characterized.

2-2-1 ZnO nanowire electrodes

Different processes for incorporation (lamination, spincoating, and spraying) of nanostructured ZnO into organic photovoltaics have been explored, and preliminary results show a marked increase in the diffuse transmission of light when compared to etched ZnO films, particularly at long wavelengths. Also, blending the nanostructures with conducting polymers (e.g. PEDOT) has been used as a way to improve the electrical properties of the films.

For P3HT:PCBM bulk heterojunction solar cells, the transparent electrode is usually comprised of ITO followed by a thin layer of PEDOT. In our devices, we laminated films cast with different ZnO nanowires to PEDOT ratio in order to create a ZnO-PEDOT composite, followed by planarization steps. This was aimed to use the PEDOT matrix for electrical conduction and the embedded ZnO nanowires for light diffusion.

For low intercalation, the light scattering is high due to the high refractive index contrast between ZnO and air, but the electrical properties of the cell are not optimal. We see a definite increase in the generated photocurrent, but charge is not efficiently harvested and we only collect all of it with a high reverse bias. Better intercalation improves the charge collection efficiency, but lowers the refractive index contrast (ZnO-PEDOT vs. ZnO-air) and the enhanced charge generation is lower.

For the optimized devices, there is a marginal increase in the power conversion efficiency when compared to control devices, with open circuit currents around 10 mA/cm^2 , which is very close to the best devices reported in literature. Further improvement of the electrical properties of the ZnO nanostructures could lead to better performance of these devices, with a negligible increase in cost or processing steps.

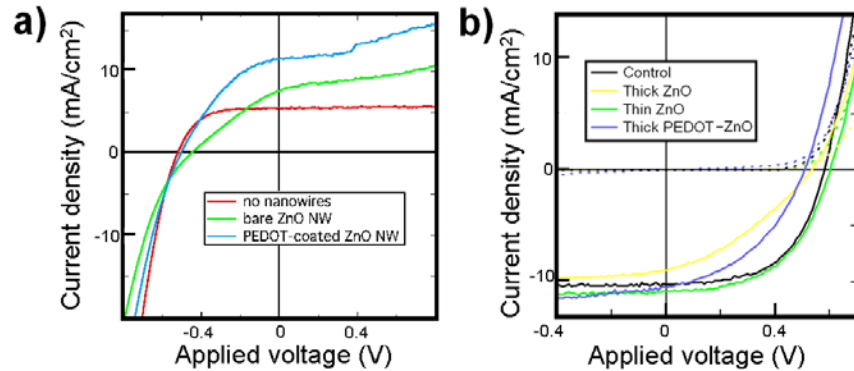


Figure 8: a) *J-V* curves for the non optimized devices, showing a marked increase in the generated photocurrent. b) Optimized devices show a lower improvement due to the compromise between electrical and optical properties.

Another way to incorporate these nanostructures into solar cells is by using them in an intermediate electrode in a tandem architecture. The performance of these devices is yet to be optimized, but initial results show promise. The electrical properties of the ZnO film must be enhanced without the need for annealing, since pre-annealed films show higher resistance which hinders device efficiency. Post-deposition annealing the ZnO films is not possible in this architecture due to the presence of organic layers.

2-2-2 Ag Nanowire Electrodes

A shortcoming of Ag NW mesh networks as TCO replacement was that the film roughness (with peak-to-valley roughness of $>2x$ the wire diameter) prevented the demonstration of high-quality devices. This problem was addressed by making composite structures consisting of a polymer (PEDOT:PSS) in which a Ag NW mesh is embedded by lamination. Scanning electron micrographs of the resulting films are shown in Fig. 9.

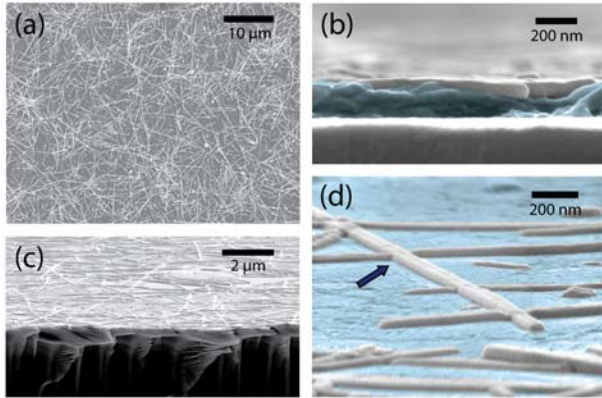


Figure 9: SEM micrographs of Ag nanowires embedded in PEDOT:PSS. Plan view (a), cross-sectional side-views (b and c) and surface view (d). The arrow points to a partially embedded nanowire.

The wires are mostly embedded in the underlying polymer film, presenting a much flatter surface to build solar cells on. As a result, we were able to construct organic solar cells whose performance is indistinguishable from those built on ITO. For these experiments, the well-known materials system P3HT:PCBM was used, resulting in 4.2% cells on both ITO and Ag NW/polymer composites. On plastic substrates, the Ag NW/polymer composites are superior to ITO because a lower sheet resistance can be obtained, resulting in an efficiency of 3.8% for cells on Ag NW anodes and 3.4% on ITO (Fig. 10).

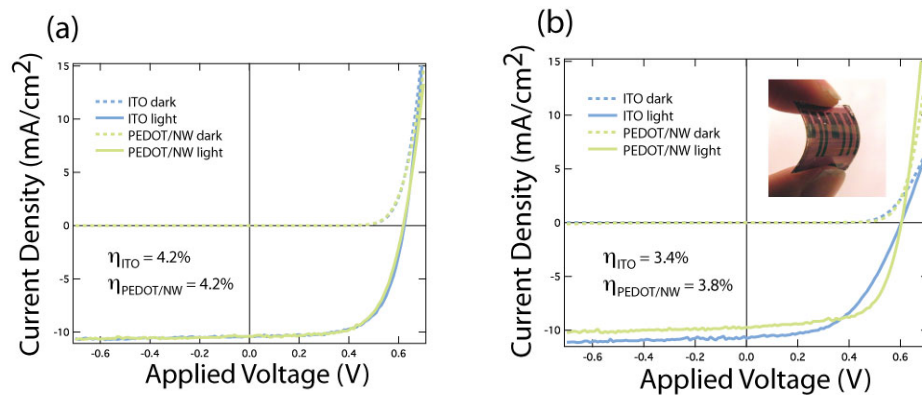


Figure 10: Comparison of the I - V characteristics of P3HT:PCBM solar cells made with Ag nanowire and ITO electrodes on glass (a) and flexible substrates (b)

Fig. 11a below compares optical transmission data for ITO and Ag NW/polymer composites, showing comparable performance. Note that the Ag NW samples have a lower sheet resistance than the ITO samples used here. An additional advantage of the Ag NW meshes over ITO (or other metal oxide TCOs) is that they are much more robust under mechanical stress. This is shown in Fig. 11b where the sheet resistance is measured as a function of the bending radius for ITO and a Ag NW mesh on 5 mil thick plastic substrates (films are under tension). The ITO film is more resistive because the plastic substrate imposes limits on the ITO sputtering conditions. The ITO film fails at a bending radius of ~ 9 mm, while the Ag NW film does not fail. Progress was also made in developing a spray-coating process to coat larger substrates with Ag NW meshes. A custom spray-coater was developed and allows for substrates up to 12" x 12" to be coated uniformly. The performance of Ag NW meshes deposited by spray-coating are comparable to those deposited using drop-casting.

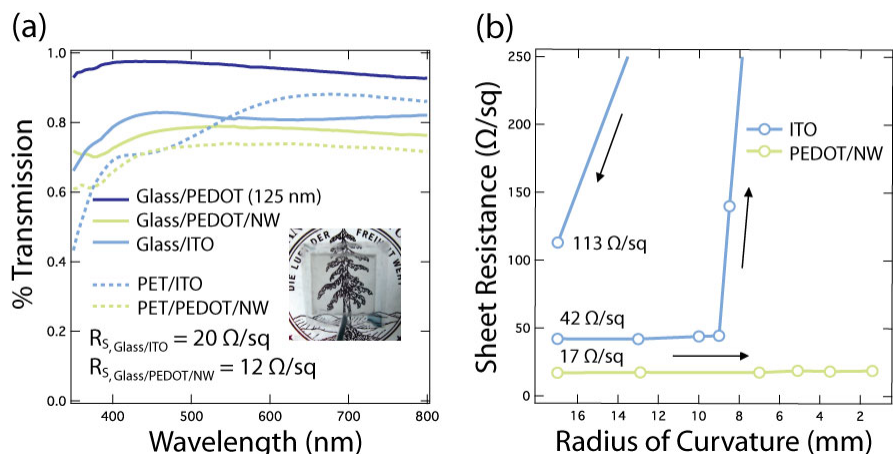


Figure 11: Optical transmission of ITO and Ag nanowire composites (a). Sheet resistance as a function of radius of curvature for ITO and Ag nanowire composites.

3. Future goals

Degeneratively doped ZnO nanowires

- Understand the defect chemistry of doped ZnO using x-ray techniques.
- Increase carrier density in doped ZnO nanowires by chemical or thermal treatments
- Study the relationship between film conductivity and wire connectivity
- Study interwire contact resistance
- Fabricate multijunction devices with ZnO interlayer electrodes

Ag nanowire meshes

- Improve electrical and optical properties
- Explore composites with ZnO nanowires
- Integrate in photovoltaic device

Semiconductor layers

- Study performance in solar cells
- Integrate with other materials

Device fabrication and characterization

- Fabricate multi-junction cell using lamination, solution processing or a combination
- Further develop simulation codes for unconstrained cells
- Optimize device design

4. Publications

1. B. D. Weil, S. T. Connor, Y. Cui “CuInS₂ Solar Cells by Air-stable Ink Rolling” *J. Am. Chem. Soc.* (in press).
2. L. Hu, H. S. Kim, J.-Y. Lee, P. Peumans and Y. Cui “Scalable Coating and Properties of Transparent, Flexible Silver Nanowire Electrodes” *ACS Nano* (in press).
3. R. Noriega, J. Rivnay, L. Goris, D. Kälblein, H. Klauk, K. Kern, L. M. Thompson, A. C. Palke, J. F. Stebbins, J. R. Jokisaari, G. Kusinski, and A. Salleo, “Probing the electrical properties of highly-doped Al:ZnO nanowire ensembles”, *Journal of Applied Physics* 107, 074312-1-7 (2010).

4. G. J. Kusinski, J. R. Jokisaari, R. Noriega, L. Goris, M. Donovan, A. Salleo, "Transmission electron microscopy of solution-processed intrinsic and Al-doped ZnO nanowires for transparent electrode fabrication", *Journal of Microscopy* 237, 443-449 (2010).
5. R. Devan, M. Marinkovic, R. Noriega, S. Phadke, A. Salleo, D. Knipp, "Light Trapping in Thin Film Silicon Solar Cells with Periodic Pyramid Texture", *Optics Express* 17, 23058-23065 (2009).
6. W. Gaynor, J.-Y. Lee and P. Peumans, "Fully Solution-Processed Inverted Polymer Solar Cells With Laminated Nanowire Electrodes," *ACS Nano*, Vol. 4 (1), 30-34 (2010).
7. J.-Y. Lee, S. T. Connor, Y. Cui and P. Peumans, "Semitransparent Organic Photovoltaic Cells with Laminated Top Electrode", *Nano Letters*, Vol. 10 (4), 1276-1279 (2010).